

Development of silicon nitride/silicon carbide composites for wood-cutting tools

F. Eblagon^a, B. Ehrle^b, T. Graule^a, J. Kuebler^{a,*}

^a Empa, Laboratory for High Performance Ceramics, CH-8600 Dübendorf, Switzerland

^b OERTLI Werkzeuge AG, CH-8181 Höri, Switzerland

Received 1 December 2005; received in revised form 10 February 2006; accepted 17 February 2006

Available online 18 April 2006

Abstract

Industrial wood-cutting inserts were produced from both Si_3N_4 - and Si_3N_4 -based ceramic matrix composites (CMC), subjected to industrial wood-cutting conditions and compared to tungsten carbide (WC). Relevant material properties for this particular application were collected and compared to the results obtained from the cutting tests. The results show that $\text{Si}_3\text{N}_4/30 \text{ wt. \% SiC}$ gives the best balance between fracture toughness and wear. An yttria/lanthana sintering aid system allows the production of a very fine-grained microstructure without decreasing the fracture toughness. Post-hipping and crack-healing operations have been shown to be of paramount importance for the survivability of the cutting edges. An extrapolation from the lifetime prediction test gives a potential lifetime for the CMC material three times that obtained from the WC.

© 2006 Elsevier Ltd. All rights reserved.

Keywords: Composites; Si_3N_4 ; SiC; Cutting tools; Wood machining

1. Introduction

Humans have been toolmakers for at least 2.5 million years, the earliest woodworking technology being a series of tools fabricated from shaped pebbles. The axe was developed during the Mesolithic, which started around 100,000 years ago. As years went past, tools for wood machining developed through major inventions such as saw cutting, abrasive planing and moulding. Today's woodworking industry requires high speeds for cutting and high quality surface finish, all in one operation, and at competitive costs.

Wood cutting is a highly demanding application for cutting materials, i.e.:

- According to experience from our industrial partner OERTLI AG, in order to obtain a high quality finish on the cut surface, the tool must have a very sharp cutting edge, i.e. the cutting edge should have a radius of $5 \mu\text{m}$ or less, ideally $1 \mu\text{m}$.
- Acids, hydrocarbons and tannins contained in the wood generate a corrosive environment in the cutting area. Oxides can

also be found in the wood, such as those of potassium, calcium, magnesium and silicon in the case of some tropical woods.¹

- High temperatures are generated at the cutting edge (between 400°C^2 and 800°C^3) and no cooling can be used in this operation apart from air since any liquid would affect the surface quality of the wood.⁴
- Wood is an orthotropic material with an inhomogeneous structure which includes knots and sand entrapments.³
- The use of wear-resistant coatings such as diamond is restricted due to the small radius required on the cutting edge. Coatings can increase the edge radius from approximately $1 \mu\text{m}$ to $15 \mu\text{m}$.⁵

The standard material used in the industry for high-volume planing and cutting of wood or wood chip panels is tungsten carbide (WC). WC is liquid phase sintered with a metallic binding phase usually formed either with cobalt, or a cobalt alloy. The amount of the metal binding phase affects the hardness, corrosion resistance, fracture toughness and rigidity of the composite.⁶ It has also been observed that wear resistance increases with increasing hardness and decreasing grain size and binder content for different WC grades.⁷

Grain size in WC grades vary between $0.3 \mu\text{m}$ and $40 \mu\text{m}$. Wood-machining grades have an average grain size of $\sim 0.5 \mu\text{m}$,

* Corresponding author. Tel.: +41 44 823 4223; fax: +41 44 823 4510.
E-mail address: jakob.kuebler@empa.ch (J. Kuebler).

which is ideal for producing sharp cutting edges for this application.⁸ WC also shows a high thermal conductivity, four to five times that of silicon nitride,⁹ which aids in dissipating heat away from the cutting edge. Due to the metallic nature of the binder phase of this composite, WC shows an outstanding fracture toughness which, coupled with the high hardness given by the tungsten carbide, allows it to deal with inclusions and knots.⁶

WC cutting tools last longer than traditional high strength steel (HSS) tools, even though HSS is preferred when a very high quality finish is required. In spite of the longer service life of WC cutting tools, the metallic binding phase in the WC composite reacts with tannic acids found in the wood. This chemical reaction is believed to leach out the cobalt binder and to leave the WC grains exposed and prone to detachment during the wood-machining operation.¹⁰

In other industries, ceramics have replaced WC and coated WC for machining applications, e.g. of grey and nodular cast iron, with increased cutting speeds and tool life being observed. Other difficulties to machine materials such as hardened steel and superalloys have also benefited from CMC cutting tools.¹¹

A high wear resistance is desired for cutting tools, and materials with high hardness, good toughness and high hot strength are most resistant to abrasive wear.¹² Silicon nitride ceramics show a higher hardness than hardmetal. Nevertheless, fracture toughness in monolithic ceramics is too low for this kind of applications. The K_{IC} of ceramics can be increased by tailoring the microstructure so that the higher hardness can be exploited. According to Huang et al.,¹³ TiN additions can increase the fracture toughness of Si_3N_4 by ~35% by different crack deflection mechanisms, although lower values have been reported by Blugan et al.¹⁴ A fracture toughness increase has also been observed when adding SiC to a Si_3N_4 matrix.¹⁵ The production of CMCs allows the use of the outstanding hardness found in ceramic materials.

It has been observed that compared to other oxides, yttria and lanthana sintering additives yield β -silicon nitride grains with the highest aspect ratio and consequently increase the fracture toughness of Si_3N_4 .¹⁶ A weaker glassy phase such as that resulting from the addition of lanthanum or neodymium promotes intergranular crack propagation which increases the apparent fracture toughness of the material.¹⁷ Furthermore, yttria/lanthana garnets (YLaG) in different compositions have been shown to produce a higher melting point glassy phase than those observed with yttria/alumina (YAG) or aluminium nitride/yttria garnets. This increase in the melting temperature increases the strength of the material at high temperatures and therefore the maximum service temperature.¹⁸

Other properties such as the thermal conductivity can be modified by tailoring either the glassy phase composition or the microstructure. It has been reported that by tailoring the glassy phase composition in liquid-phase sintered silicon carbide, the thermal conductivity can be doubled.¹⁹ Furthermore, a reduction on the glassy phase content increases the thermal conductivity of a composite, k_c .

The thermal conductivity also increases steeply with increasing grain size until it reaches an almost constant value above a

certain critical grain size. However, as mentioned, a small radius is necessary at the cutting edge in order to produce a high quality finish on the wood surface. In order to produce a cutting radius of 1 μm , the grain size of the starting material should be 1 μm or smaller; therefore, a compromise between the mechanical and thermal properties of the material and the cutting radius must be found.

The aim of this study was to develop silicon nitride-based composite materials for industrial wood-machining cutting tools and to compare these materials with tungsten carbide with respect to both mechanical properties and tool lifetime.

2. Experimental procedure

2.1. Materials

Two commercial reference materials were used in the context of this study. The first material was a MG18 hardmetal from CERATIZIT Horb GmbH, Germany, which is used as a standard wood-cutting tool material by different companies. The composition of this material is approximately 90 wt.% WC and 10.0 wt.% Co, and it was supplied as off-the-shelf reversible knives with two cutting edges.

The second material was a commercial grade silicon nitride. This material was supplied as a 250 mm diameter disc by FCT Ingenieurkeramik GmbH, Germany. It was produced from hot-pressed silicon nitride SN10 from UBE, Japan, with 2.0 wt.% alumina and 1 wt.% yttria as sintering aids.

A series of Si_3N_4 -based CMCs were produced tailored to this particular application. The starting matrix powder for the CMC was micron-sized silicon nitride grade M11 from H.C. Starck, Germany. As the second phase, two different ceramics were used: Either titanium nitride grade C and silicon carbide grade UF25, both from H.C. Starck, Germany.

Two different sintering aids were used to densify the silicon nitride. The first system was an yttria–alumina garnet (YAG), 5.0 wt.% and 3.0 wt.%, respectively. The second system was a lanthana–yttria garnet, also with 5.0 wt.% and 3.0 wt.%, respectively. The alumina used was grade CT 3000 supplied by Alcoa Germany, the yttria was grade C from H.C. Starck, Germany, and the lanthana was obtained from Auer Remy, Germany.

The powder mixtures prepared are summarised in Table 1. The particle sizes were measured using a Beckman Coulter LS 230 particle size analyser with polarization intensity differential scattering (PIDS). A typical particle size distribution chart for the powder mixture after milling is shown in Fig. 1.

The powders were mixed in isopropanol and milled in a planetary mill at 200 rpm for 4 h. The milling media used were 3 mm diameter alumina balls inside a 500 ml container with an alumina lining. After milling, an isopropanol solution of Mowital B30T PVB binder from Clariant, Germany, was added and the ceramic slurry was mixed for a further 5 min. The amount of binder used was 0.5 wt.% for all the powder mixtures. The mixture was then dried in a vacuum rotating dryer (Büchi Rota Vapor, Switzerland) and sieved to 100 μm .

Sintering was carried out in a laboratory-size hot-press built by Thermal Technology Co. USA, and refurbished by FCT Anla-

Table 1
Composition of the CMC powder mixtures

| | STN–YAG | STN–YLaG | SNC–YAG | SNC–YLaG |
|---|---------|----------|---------|----------|
| Si ₃ N ₄ (wt.%) | 70.0 | 70.0 | 70.0 | 70.0 |
| TiN (wt.%) | 30.0 | 30.0 | – | – |
| SiC (wt.%) | – | – | 30.0 | 30.0 |
| Particle size of the mixture after milling (<i>d</i> ₅₀ [μm]) | 0.4 | 1.1 | 0.7 | 1.1 |

STN: silicon nitride + titanium nitride composite; SNC: silicon nitride + silicon carbide composite; YAG: yttria–alumina garnet; YLaG: yttria–lanthana garnet.

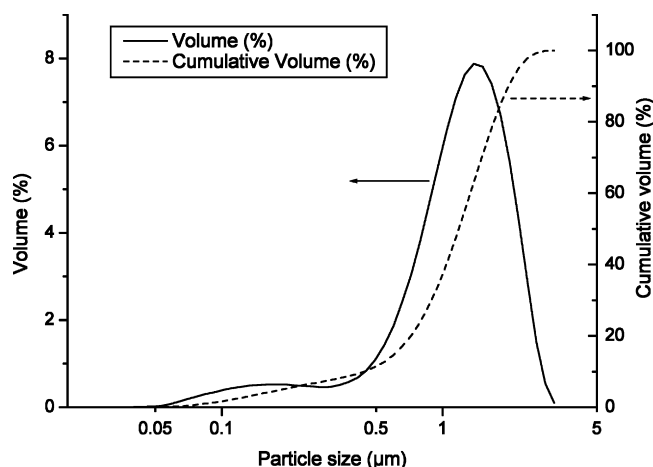


Fig. 1. Particle size distribution for Si₃N₄ + 30 wt.% SiC powder.

genbau GmbH, Germany. The CMCs were sintered at 1800 °C and 30 MPa pressure for 30 min in either nitrogen or argon atmosphere.

A summary of the materials used and their sintering conditions is given in Table 2.

A differential dilatometer was used for measuring the sintering behaviour of the cold-pressed powders under different atmospheres. The equipment used was a Sinter-dilatometer 802

Table 2
Sample matrix

| Samples | Material | Temperature (°C) | Dwell (min) | Atmosphere |
|---------------------------------|---|------------------|---------------|----------------|
| Short-run test | | | | |
| S1 | WC | | | |
| S2 | STN–YAG | 1800 | 30 | N ₂ |
| S3 | STN–YAG | 1800 | 70 | N ₂ |
| S4 | STN–YAG | 1800 | 20 | N ₂ |
| S5 ^a | STN–YAG | 1800 | 30 | N ₂ |
| S6 | STN–YLaG | 1800 | 30 | N ₂ |
| S7 | SNC–YAG | 1800 | 30 | N ₂ |
| S8 | Unreinforced Si ₃ N ₄ | 1750 | Not available | N ₂ |
| Lifetime prediction test | | | | |
| A1–A5 | WC | | | |
| B1–B5 | SNC–YAG | 1800 | 30 | N ₂ |
| C1–C5 ^a | SNC–YAG | 1800 | 30 | N ₂ |
| D1–D5 | STN–YLaG | 1800 | 30 | N ₂ |
| E1–E5 ^b | SNC–YLaG | 1800 | 30 | N ₂ |
| F1–F5 ^c | SNC–YLaG | 1800 | 30 | Ar |

^a Post-sintered for 4 h @ 1200 °C.

^b Post-sintered only sample E5 for 4 h @ 1200 °C in air.

^c Post-sintered for 4 h @ 1200 °C in argon.

S from Bähr–Thermoanalyse GmbH, Germany. A graphite furnace with a graphite inert sample for comparison was used for the measurements. The temperature was ramped from room temperature to 2000 °C at 5 °C min^{−1} and then cooled down at the same rate with no dwell. The atmospheres used were both argon and nitrogen. Two samples of each sintering aid systems were measured in both atmospheres.

2.2. Mechanical properties and chemical resistance

The indentation fracture (IF) toughness was measured using a Vickers hardness indenter according to the JIS-R 1607 standard for direct comparison purposes only. The hardness was evaluated using a Vickers diamond indenter according to the ENV 843-4 standard. The diagonals of the impressions were measured using an optical microscope with a XY-table to the nearest 1 μm, which gave an average measurement error of ±0.5%.

The samples were tested for weight changes after 2 h and 10 h immersions in a 0.1 M solution of tannic acid at 60 °C. The tannic acid was supplied as a high purity powder by Fluka AG, Switzerland. The Vickers hardness after immersion for 2 h was also measured.

2.3. Cutting tests

For the production of the cutting inserts, sintered discs, 20.0 mm in diameter and 2.5 mm in thickness, were pre-machined using a D126 grit diamond wheel. The inserts were then machined to their final dimensions according to Fig. 2 using

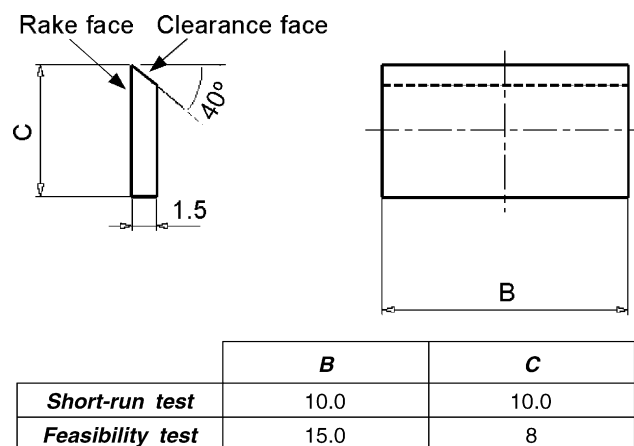


Fig. 2. Final dimensions CMC cutting tools (not to scale). All the dimensions are in millimeter.

Table 3
Cutting condition used during the cutting tests

| | Short-run cutting test | Lifetime prediction test |
|------------------------------|------------------------|--------------------------|
| Rotating spindle speed (rpm) | 8000 | 10000 |
| Tool diameter (mm) | 150 | 140 |
| Cutting speed (m/s) | 62.8 | 73.3 |
| Cutting depth (mm) | 5 | 4 |
| Feed rate (m/min) | 12 | 15 |
| Feed rate per tooth (mm) | | 1.50 |
| Average chip thickness (mm) | | 0.25 |

a three-stage polishing operation with 15 μm , 6 μm and 1 μm diamond pastes.

Two different cutting tests were carried out. A short cutting test which was aimed at evaluating the survivability of the cutting edge under normal industrial wood-cutting conditions with lengths of cut below 5 m. Samples S1 to S8 were used for this test. A second longer test was carried out in order to predict the potential lifetime of the cutting tools. This test was carried out also under normal industrial wood-cutting conditions with cutting distances between 50 m and 500 m. Samples A to F were used in this test. The cutting conditions used are summarised in Table 3.

The short-run cutting test was carried out on a GF Brugg type HAC machine, Switzerland, with assisted feed. The cutting inserts were tried both in a soft wood (spruce) and a hard wood (beech) in the short-run tests. Additionally, samples S2 and S5 were used to cut between 2 m and 5 m of wood with knots.

The lifetime prediction tests were carried out in a 200 Series CNC processing centre from HOMAG BAZ, Germany. A purpose-built tool was used that could hold both the ceramic knives and the standard tungsten carbide knives. These tests were carried out to cutting distances of 50 m, 100 m, 200 m, 300 m and 500 m. The wood used in the cutting tests was a mosaic-like panel. The panel consisted of glued beech pieces with alternating fibre orientation. The wood samples were planed to a thickness of 12 mm, and cut to 2.0 m length by 1.0 m width.

After the lifetime prediction test, sample E-5 was post-sintered in air at 1200 °C for 4 h and hot isostatic pressed at 1200 °C for 4 h in a 1950 bar nitrogen atmosphere in order to evaluate the influence of the hiping process on the lifetime of the cutting tools.

2.4. Tool characterization

After checking the tools for macroscopic defects, the tools were analysed using a VEGA Tescan TS5136MM scanning electron microscope (SEM) to observe the apparent radius of the cutting edge and defects created during the wood-machining operation.

One tool of each ceramic composition was polished using 15 μm , 6 μm and 1 μm diamond paste. The tools were then etched using CF_4 in a PVD magnetron to reveal the microstructure. The microstructure was observed in the scanning electron microscope to determine the average grain size and the porosity.

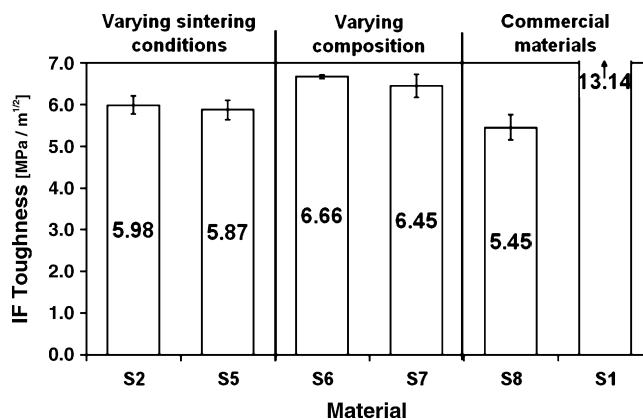


Fig. 3. Indentation fracture (IF) toughness for materials produced under different conditions (according to Miyoshi JIS-R 1607 standard).

In order to predict the potential lifetime from the feasibility proof test, the tools were cut and their cross-sections polished and analysed in the electron microscope in order to measure the change in radius of the cutting edge. The measurement of the wear on post-sintered inserts proved to be difficult due to the existence of a surface silicon oxide layer on the cutting edge. This layer was removed from the cutting edge during the cutting operation, thereby reducing the radius at the cutting edge and effectively sharpening the tool. In order to produce relevant results, the measurements on the cutting inserts were made by taking the interface between this amorphous layer and the polycrystalline material as the actual face of the tool.

Selected wood samples obtained from the lifetime prediction tests were analysed using an AltiSurf 500 profilometer, and three profiles were obtained from each sample in order to compare the surface finishes on the wood.

3. Results

3.1. Mechanical properties

The results for the indentation fracture toughness determination are summarised in Fig. 3. These values should not be taken as absolute values, but only as reference for direct comparison with other values obtained under similar conditions.

The results from the Vickers hardness and the influence of the tannic acid attack on this material property are plotted in Fig. 4. The variation in the hardness values after 2 h immersion in tannic acid for both tungsten carbide and ceramic materials were observed to be within the standard deviation for the measurements as shown in Fig. 4. The weight changes of the samples immersed in tannic acid were found to be within the measurement uncertainty of the balance.

3.2. Edge integrity tests (short-run test)

Most of the materials tested showed no influence of the type of wood being machined (soft or hard) on the survivability of the cutting inserts.

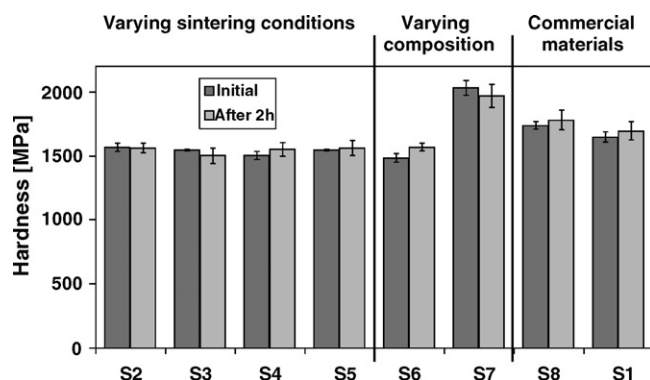


Fig. 4. Vickers hardness (HV30) for different materials, and influence of tannic acid immersion on hardness.

No damage could be observed on the cutting edge of the benchmark S1 (WC) insert. Wood depositions were visible on the rake face, probably promoted by the rough surface finish. Visible damage could be observed on the cutting edge of the commercial reference ceramic material insert S8 (Si_3N_4) when removed from the machine. A detailed view of the cutting edge is shown in the micrographs in Fig. 5. Severe edge chipping can be observed along the length of the insert. The quality of the machined wood was also affected and scratches could be observed along the width of the cut surface.

Deep machining grooves were visible on the rake surface of the as-received S8 insert when observed under the SEM. These machining marks can act as stress concentrators on the cutting edge. Consequently, the surface of the cutting edge on a second insert made from the ceramic reference material was polished with 15 μm , 6 μm and 1 μm diamond paste in order to achieve a surface finish similar to that obtained in the CMCs, and the cutting test was repeated. The result of the test was similar to that of the as-received unpolished insert, though the edge cracking was not as severe.

Chipping damage was observed on the cutting edge of the S3 insert. Even though localised damage was observed in this tool, the cutting edge radius remained constant. With exception of this insert, samples S2 to S7 revealed no damage, either at low or high magnification, incurred during the wood-machining stage. The rake face of the tools was clean and free of markings. No material seems to have been removed by the wood machining.

No damage was visible on the ceramic cutting inserts used to cut wood containing knots. The quality of the cut surfaces was

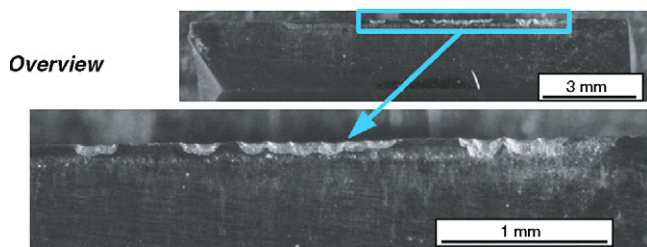


Fig. 5. Micrographs of cutting edge insert S8 showing machining damage on clearance face/optical microscopy.

also good when compared with the cut surface obtained with the commercial tungsten carbide knives. Wood with knots was machined using ceramic matrix composite inserts both with and without post-sintering.

3.3. Cut surface quality

For the purpose of quality control of the surface finish, one softwood sample cut with a commercial WC insert Type 217/015 from OERTLI AG, Switzerland, was used as a benchmark for finish quality. Softwood was chosen as a reference because it is more difficult to obtain a good quality surface on this material due to the appearance of fibres perpendicular to the surface if the radius of the cutting tool is not below a certain threshold. This threshold is determined by the wood type.²⁰ The cut surfaces obtained with the ceramic inserts were compared to the benchmark by touch, optical microscopy and profilometry. Due to lack of standards for the quality evaluation of the wood surface,²¹ tactile comparison by the machine operator is currently still the quickest and most widespread quality criterion. The comparison by touch of the wood surface quality between the WC inserts and the CMC inserts gave satisfactory results.

Profilometry was carried out on wood samples from the above-mentioned cutting inserts to quantitatively assess the quality of the surface finish. The average roughness (R_a) was used for comparison between the surface produced with the commercial WC insert and a CMC insert. The R_a for both samples was found to be very similar. The R_a measured for the WC insert was 4.50 μm and 4.77 μm for the CMC insert.

3.4. Lifetime prediction tests

Before the test, the tools were checked optically for defects on the cutting edge and the apparent cutting edge radii were measured. The apparent cutting edge radii were all below 5 μm and most of the tools were very close to the ideal 1 μm required to produce a good quality finish on a wood surface.

The tests were carried out in order to determine the wear on the cutting edge at different lengths of cutting. When the first marks were observed on the wood surface caused by chipping of the tool edge, the distance cut by the tool would be recorded as the *acceptable quality cutting distance*. If the chipping extended over the length of the cutting edge, or if the tool failed during the test, it would be rated as having *not survived*. The survivability results are summarised in Fig. 6.

As can be seen from the dilatometry results in Fig. 7, argon sintering was observed to give higher shrinkage rate and lower sintering temperature compared to sintering in nitrogen atmosphere. This is evidenced by a displacement of the shrinkage peaks to lower temperatures for the argon sintering atmosphere curves. The total shrinkage, represented by the integrated peak area, is also higher under argon than under nitrogen. This result holds for both sintering additive systems. However, despite the higher density, Fig. 6 shows that the tools sintered under an argon atmosphere (sample F) showed no improvement in the survivability of the cutting edges.

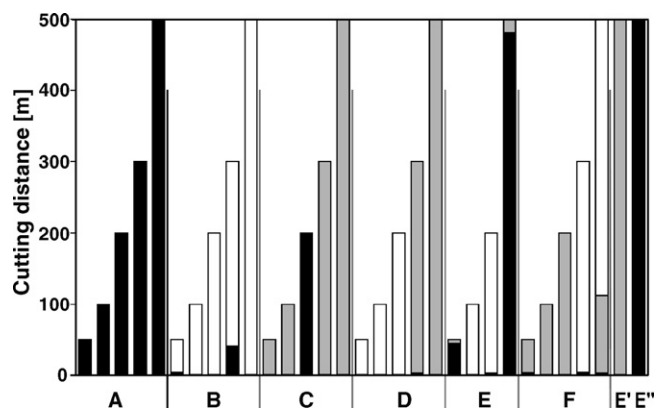


Fig. 6. Survival data of tested cutting tools. E' corresponds to sample E5 post-sintered and hipped. E'' corresponds to E' resharpened. White stands for not survived, grey symbolises survived but surface quality not acceptable and black represents distance cut with good quality.

Insert E5 was post-hipped and used to attempt a cutting test of 500 m to observe the influence of this operation on the survivability of the cutting edge. This insert survived the 500 m test with no defects on the cutting edge. However, the quality obtained was judged not to be as good as that obtained with the tungsten carbide inserts. This was due to the processing route: The tool was first sharpened, then annealed in air and finally post-hipped in nitrogen, thereby creating a thick silicon oxide layer on the surface of the tool which made the edge of the cutting insert blunt. This layer was later observed under the electron microscope to be between 4 μm and 6 μm thick. The apparent radius of the cutting edge on this tool was estimated to be $\sim 9 \mu\text{m}$.

The cutting edge of this insert was subsequently resharpened by polishing only the clearance face, leaving the rake face with the silicon oxide layer on it. The tool completed 500 m of cutting distance under industrial cutting conditions and the quality obtained was similar to that achieved when cutting with new tungsten carbide tools. The tool showed damage on the cutting edge after the first cut was made at the edge of the wood, though this could be due to previously existing defects since no further damage developed during the remainder of the 500 m test.

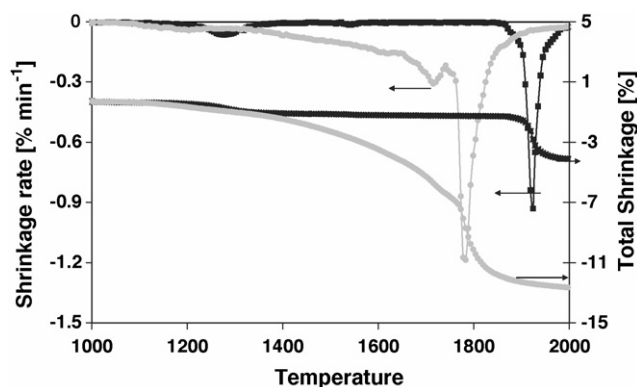


Fig. 7. Dilatometry results for $\text{Si}_3\text{N}_4/30 \text{ wt.}\% \text{ SiC}$ in N_2 and Ar atmospheres. Black symbols belong to nitrogen atmosphere sintering and grey data points represent argon atmosphere sintering.

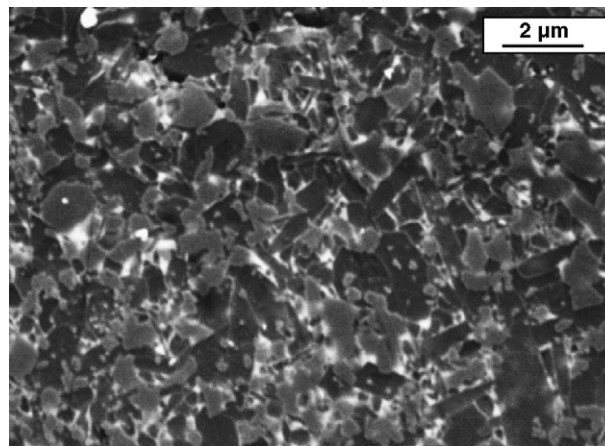


Fig. 8. Microstructure from sample E4. Secondary electron. Brighter grey areas correspond to SiC grains and darker grey elongated areas correspond to silicon nitride beta grains.

3.5. Microstructure

The microstructure of polished and etched surfaces of the inserts were analysed with the SEM and a typical microstructure for the $\text{Si}_3\text{N}_4/\text{SiC}$ composites produced can be seen in Fig. 8. An image analysis software package was used to measure the average particle size and the porosity. The average grain size was observed to be below 1 μm for all of the samples. Fig. 9 shows that the porosity has a direct influence on the survivability of the cutting inserts used in this test, i.e. survivability is increased with increasing density. This was true for most of the materials, the exception being the case when argon was used as a sintering atmosphere, where no correlation between the density of the samples and the survivability of the tools was found.

The microstructures of the materials containing the yttria–alumina and the yttria–lanthana garnet were compared in order to evaluate the influence of the sintering additives on the aspect ratio of the $\beta\text{-Si}_3\text{N}_4$ grains. The aspect ratio of the grains showed a shift to higher values for the yttria–lanthana system as shown in Fig. 10.

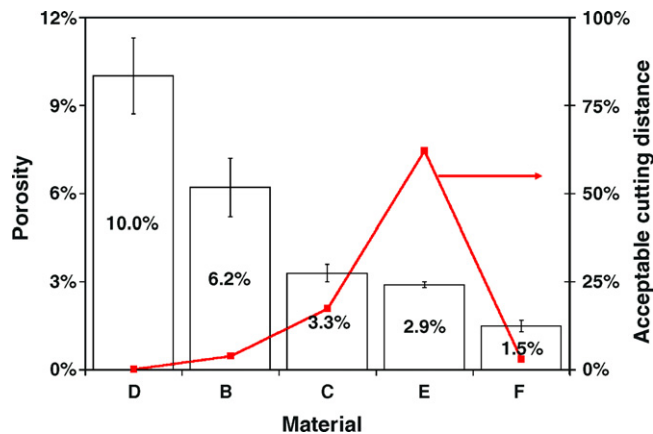


Fig. 9. Apparent porosity and acceptable quality cutting distance as a function of insert composition. Samples B–E sintered in nitrogen atmosphere. Sample F sintered in argon atmosphere.

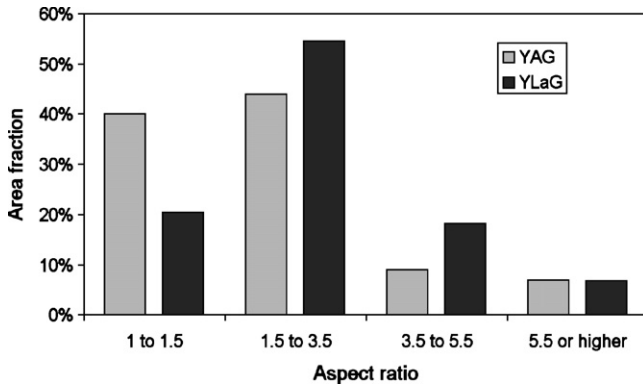


Fig. 10. Aspect ratio comparison for the sintering additive systems (YAG = sample B2, YLaG = sample E4).

Table 4 shows the relative density obtained from hot-pressing different materials under similar conditions. SiC-reinforced Si_3N_4 (samples B, C and E) exhibited larger shrinkage rates than the TiN-reinforced material (sample D).

3.6. Tool wear

The value used to predict the potential lifetime of the cutting tools was the radius at the cutting edge. The limiting value for the radius of the cutting edge that will predict the end of the

Table 4
Relative density and grain size

| Series | Relative density (%) | Average grain size (μm) |
|--------|----------------------|--------------------------------------|
| B | 93.8 (± 1.0) | 0.42 (± 0.09) |
| C | 96.7 (± 0.3) | 0.52 (± 0.14) |
| D | 90.0 (± 1.3) | 0.70 (± 0.11) |
| E | 97.1 (± 0.1) | 0.41 (± 0.06) |
| F | 98.5 (± 0.2) | 0.37 (± 0.05) |

lifetime of the insert is dependent on the process and the machine operator. In order to compare the lifetime of the materials used for the cutting inserts analysed in this test, a maximum cutting edge radius of $5 \mu\text{m}$ was set as the end of the life for these tools. Fig. 11 shows a cross-section of the cutting edges as observed in the secondary electron mode (SEM) before and after the 500 m cutting test. The results of the SEM analysis are summarised in Table 5.

Using the values obtained from the micrographs summarised in Table 5, a plot of cutting edge radius versus cutting distance can be generated to predict the approximate lifetime of the cutting inserts. From an extrapolation of the linear fit to the cutting radius data in Fig. 12, an estimated service life of 1500 m can be expected for the WC and 5000 m for the CMC tool. The linear fit does lead to conservative values since typical values for WC cutting tools are between 1000 m and 5000 m, depending

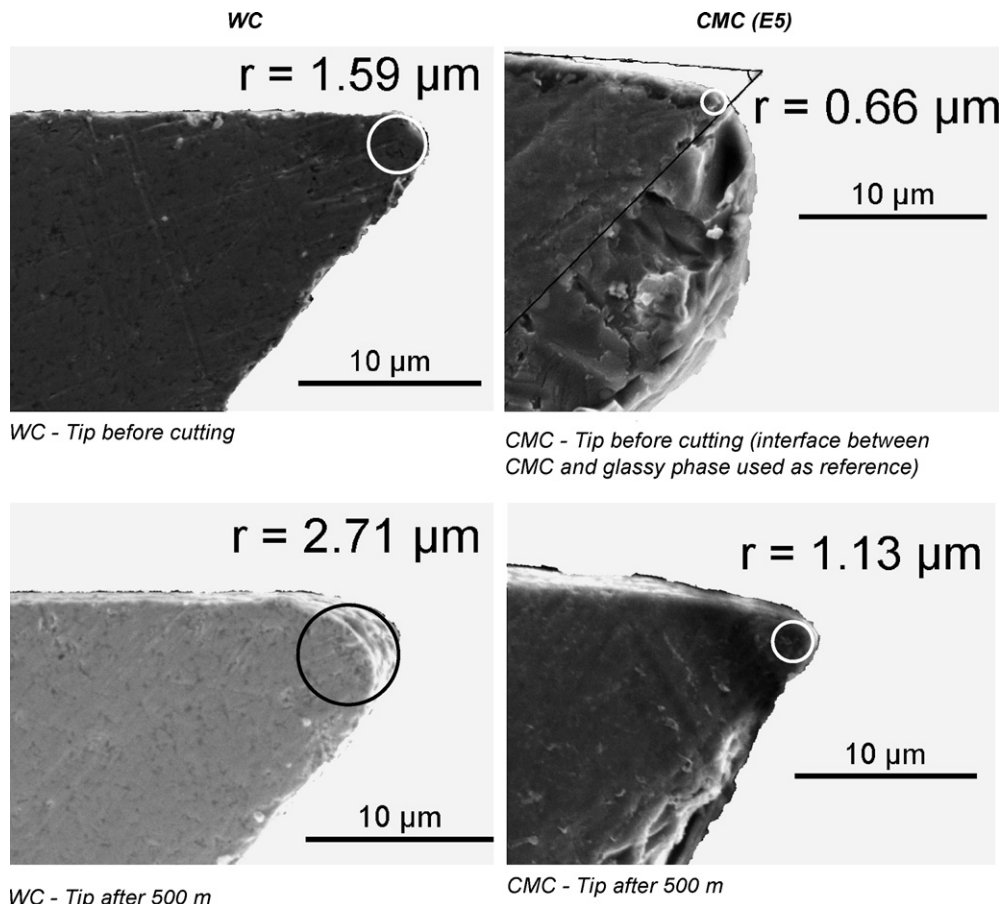


Fig. 11. Cross-section of the cutting edges at different cutting distances for WC and E5 CMC inserts.

Table 5
Tool wear in optimised cutting tools

| Cut distance (m) | Cutting edge radius (μm) | |
|------------------|---------------------------------------|---------------|
| | WC | CMC |
| 0 | 1.59 | 0.66 |
| 100 | 1.79 | Not available |
| 200 | 1.75 | Not available |
| 300 | 2.39 | Not available |
| 500 | 2.71 | 1.13 |

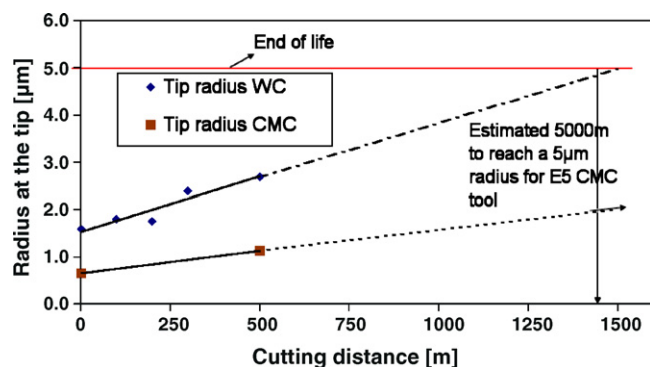


Fig. 12. Radius at the cutting edge vs. cutting distance—linear extrapolation for WC and E5 CMC inserts. Solid lines represent linear fits and dashed lines represent extrapolations.

on the application and the operator. The wear in wood-cutting tools has been observed to follow a power law,²² however, not enough data points were available to apply this model.

4. Discussion

4.1. Toughness

The indentation method did not show a strong influence of the CMC formulations on the indentation fracture toughness of the materials produced. The highest fracture toughness was obtained using lanthana and yttria as sintering aids and titanium nitride as a secondary reinforcing phase. The microstructure produced with this sintering aid system showed a shift of the aspect ratio of the β -grains towards higher values, which has been widely reported in the literature to produce tougher materials. A high fracture toughness compared to the TiN-reinforced material was observed when using silicon carbide as a secondary phase with similar sintering conditions and sintering aids. A higher toughness could be expected for the Si_3N_4 –SiC composite when combined with the yttria–lanthana glassy phase whilst still retaining a high hardness.

The YLaG produced a higher aspect ratio β - Si_3N_4 grain microstructure than the YAG. A fine microstructure ($\sim 0.5 \mu\text{m}$ average grain size) was obtained for this material under the aforementioned sintering conditions. In spite of this having been reported in the literature as being detrimental to the mechanical properties of the Si_3N_4 materials, a small grain size is required in order to produce a sharp cutting edge.

4.2. Hardness

The hardness of the materials was also influenced by the composition, but no influence of the sintering conditions could be found. Varying dwell times and post-sintering operations yielded similar hardness values. On the other hand, silicon carbide-reinforced materials showed an increase of 15% in hardness compared with the unreinforced silicon nitride. This result is expected since SiC is $\sim 50\%$ harder than Si_3N_4 . Titanium nitride additions reduced the hardness when compared with the reference material, showing good agreement with the values reported by Gogotsi.²³ Tungsten carbide showed a hardness $\sim 25\%$ smaller than that observed for the silicon carbide-reinforced silicon nitride. This would be expected to improve the wear resistance of the ceramic when compared to the tungsten carbide tool.

4.3. Tannic acid corrosion

No changes could be observed in either the hardness, or the weight loss of the tested samples after immersion in tannic acid solution for 10 h. An observable weight loss has been previously reported though only for a cobalt sample immersed 10 h in a 0.1 N tannic acid solution at 60°C .¹⁰ It is believed that the chemical attack of the cobalt binding phase in hardmetal inserts is limited to a depth equal to the grain size of the tungsten carbide, which in the current case is on the order of $0.5 \mu\text{m}$ and therefore below the measuring accuracy of the test.

4.4. Cutting test

The as-supplied tools produced from the commercial reference ceramic did survive the cutting test, but the cutting edges were severely damaged. This could initially be attributed to the machining operation used to prepare the inserts since the tools showed deep machining marks on the surface, which could have acted as stress concentrators. A rough machining procedure could have also created cracks on the surface of the material that would have had to be removed by further machining or healed via an annealing operation. The grinding direction has also been reported to have a strong effect on the strength of machined parts, particularly for silicon nitride.²⁴ The finished tools supplied were re-sharpened using the same processing conditions used for the CMC tools and a subsequent reduction of the chipping of the cutting edges was observed. Nevertheless, the defects induced on the cutting edge were still large and the cut surface of the wood was covered with tracks induced by this damage. As a consequence, material S8 was not used for the survival tests. This premature failure is believed to be related to the lower fracture toughness of the unreinforced material.

Only one CMC material, S3, showed defects on the cutting edge after the test. This material had a longer dwell time during the sintering stage and was expected to show a higher fracture toughness. The fracture toughness was measured using the IF method and did show an increase when compared to the base material, S2, though the ratio between the length of the indentation diagonal and the length of the cracks for those measurements

was below the threshold required by the test standard. Nonetheless, the chipping was localised and the rest of the cutting edge remained sharp.

No significant change in the radius of the cutting edges could be observed in the CMC tools used in the short-run cutting tests. The machining of knotted wood showed no impact either on the cutting edge, or in the surface quality of the wood in the region adjacent to the knots.

4.5. Surface quality of the wood

The surface of the wood obtained with the CMC tools was deemed to be of similar quality by touch as the quality of the surface obtained with the hardmetal inserts, even for softwood samples. A standard for the measurement of the wood surface smoothness has not yet been established, though both visual and tactile methods are currently in use.^{21,25} The profilometry results gave similar R_a values ($<5\text{ }\mu\text{m}$) for both hard and soft wood samples, with both tungsten carbide and CMC inserts. These values were found to be in good agreement with R_a reported in the literature for planed wood ($10\text{ }\mu\text{m}$ or less).²⁵ Wood fibre pullout was observed on the wood cut with the commercial reference ceramic material (S8) during the short-run cutting tests. This could be attributed to a blunt cutting edge, even though a definition of a blunt tool should be associated with the wood species to be cut, the angle between the cutting direction and the wood-grain orientation, and the particular operation. The other samples showed surface finishes free of noticeable wood fibre pullout and tracks.

4.6. Lifetime prediction tests

A direct relationship was found between the survivability of the cutting inserts and the porosity present in these tools. The highest porosity found in the D series ($\text{Si}_3\text{N}_4/\text{TiN}$) CMC tools was also linked to the lowest acceptable quality cutting distance in the whole test, even though this material showed the highest indentation fracture toughness of the tested ceramics. An increase in acceptable quality cutting distance was observed with decreasing porosity, therefore highlighting the importance of the optimisation of the sintering process and the possible need for a post-HIP operation.

An exception to this was observed with the F series ($\text{Si}_3\text{N}_4/\text{SiC}$ –YLaG) sintered in argon. The use of argon as a sintering atmosphere for silicon carbide has been observed to inhibit the production of silicon oxide, thus modifying the oxygen content in the glassy phase. The oxygen content in the glassy phase affects the properties of the material, including the viscosity of the glassy phase at high temperatures^{26,27} and would thus improve the sinterability of this material and result in a lower porosity. In fact, the use of argon atmosphere has been reported to improve the sinterability of liquid phase sintered silicon nitride.²⁸ Nevertheless, the use of argon as a post-sintering atmosphere for silicon nitride has been observed to promote the formation of clustered equiaxed grains, and reduction of large beta grains²⁹ which would render the material more brittle. A large drop in strength and oxygen content was also found in sili-

con oxynitride fibres annealed in argon atmosphere.³⁰ This was linked to the change in chemical composition and crystallisation ability of the silicon oxynitride material. Even though a drop in strength in the glassy phase has been linked to an increase in the fracture toughness of silicon nitride due to a change from transgranular to intergranular fracture mode,³¹ it remains to be assessed to which extent this is true for the system studied in this project.

5. Conclusions

In this study, silicon nitride-based ceramic matrix composites have been shown to have the potential to be used as material for industrial wood-cutting inserts.

- An extrapolation of the wear results have predicted a lifetime for the CMC cutting inserts three times that of the tungsten carbide inserts.
- The produced CMC tools have been shown to be able to cut 500 m in rough wood-machining conditions, providing similar quality of the wood surface as a standard tungsten carbide tool. The defects developed during the cutting operation were found to be of similar magnitude to those found on standard hardmetal tools.
- The cutting edges have been proven to withstand industrial wood-cutting conditions. The cutting edges were not affected by cutting wood with knots or glued wood.
- The production of ceramic cutting tools featuring cutting edges with a 50° wedge angle and radii between $1\text{ }\mu\text{m}$ and $2\text{ }\mu\text{m}$ has been proven to be feasible. The machining defects on the cutting edge of the CMC tools have been found to be of similar size to those found on standard WC cutting inserts.
- Elimination of porosity was shown to be critical and the use of a post-sintering operation has been proven to be necessary to produce reliable cutting tools for this application, though an optimised sintering-annealing process has yet to be developed.
- An optimised formulation for this application has been obtained with silicon carbide as the second phase. The SiC provides high hardness and improves the fracture toughness of the silicon nitride material and it may also have increased the thermal conductivity of the material. Furthermore, a glassy phase with a high melting temperature promotes the formation of high aspect ratio silicon nitride beta grains, giving a high fracture toughness.

Acknowledgements

The authors would like to thank Mr. Alvarez and the rest of the workshop team at Empa for their great assistance with the machining of the CMC cutting tools and fabrication of essential tooling. The authors are also grateful to Dr. Richter and Mr. Heer from the Wood Department at Empa and OERTLI AG for very helpful discussion and input in wood surface finishes and support for the execution of the in-house cutting tests. Many thanks go to Ms. Guseva and Mr. Feuz from Empa Dübendorf and Thun for their assistance with the wood surface characterisation. The

authors also wish to thank the Berner Fachhochschule in Biel for their assistance in carrying out the lifetime prediction tests. Part of this work was supported by the Swiss Commission for Technology (CTI) under contract number 6894.2 IWS-IW.

References

1. Fengel, D. and Wegener, G., *Wood—Chemistry, Ultrastructure, Reactions*. Walter de Gruyter, Berlin, 1984, pp. 34–35.
2. Sheikh-Ahmad, J. Y., Lewandowski, C. M., Bailey, J. A. and Stewart, J. S., Experimental and numerical method for determining temperature distribution in a wood cutting tool. *Exp. Heat. Tran.*, 2003, **16**, 255–271.
3. Stewart, H. A., High temperatures wear tools when wood machining. *Mod. Woodworking*, 1993, 1–4.
4. Costes, J.-P. and Larricq, P., Towards high cutting speeds in wood milling. *Ann. Forest. Sci.*, 2002, **59**, 857–865.
5. Flöter, A. and Gluche, P., Verbesserung der Schärfe diamantbeschichteter Hartmetallklingen. *Industrie Diamanten Rundschau*, 2004, **38**(II), 110–112.
6. Schneider, S. J., *Engineered Materials Handbook (Vol. 4)—Ceramics and Glasses*. ASM International, 1992, pp. 808–810.
7. Sheikh-Ahmad, J. Y. and Bailey, J. A., Wear characteristics of some cemented carbides in machining particleboard. *Wear*, 1999, **225–229**, 256–266.
8. Prakash, L. J., Application of fine grained tungsten carbide based cemented carbides. *Int. J. Refract. Met. H.*, 1995, **13**, 257–264.
9. Schneider, S. J., *Engineered Materials Handbook (Vol. 4)—Ceramics and Glasses*. ASM International, 1992, pp. 808–815.
10. Bailey, J. A., Bayoumi, A.-M. and Stewart, J. S., Wear of some cemented carbide tools in machining oak. *Wear*, 1983, **85**, 69–79.
11. Schneider, S. J., *Engineered Materials Handbook (Vol. 4)—Ceramics and Glasses*. ASM International, 1992, pp. 969–972.
12. Askeland, D. R. and Phulé, P. P., *The science and engineering of materials (4th ed.)*. Brooks/Cole-Thomson Learning, Pacific Grove, CA, 2003, pp. 971–972.
13. Huang, J.-L., Lee, M.-T., Lu, H.-H. and Lii, D.-F., Microstructure, fracture behaviour and mechanical properties of TiN/Si₃N₄ composites. *Mater. Chem. Phys.*, 1996, **45**, 203–210.
14. Blugan, G., Hadad, M., Janczak-Rusch, J., Kuebler, J. and Graule, T., Fractography, mechanical properties, and microstructure of commercial silicon nitride-titanium nitride composites. *J. Am. Ceram. Soc.*, 2005, **88**(4), 926–933.
15. Hong, J., Jingyan, H. and Zhihua, X., Study of SiC particle reinforced and toughened silicon nitride base ceramic cutting tool material. *Rare Metal Mat. Eng.*, 1999, **28**(3), 182–185.
16. Schneider, S. J., *Engineered Materials Handbook (Vol. 4)—Ceramics and Glasses*. ASM International, 1992, pp. 814–816.
17. Hoffmann, M. J., Gu, H. and Cannon, R. M., Influence of the interfacial properties on the microstructural development and properties of silicon nitride ceramics. In *Materials Research Society Symposium Proceedings*, 2000, pp. 65–74, p. 586.
18. Bellosi, A. and Babini, G. N., Effects of raw powders on microstructure and properties of Si₃N₄-based ceramics. *Key Eng. Mat.*, 1999, **161–163**, 203–208.
19. Zhou, Y., Hirao, K., Yamauchi, Y. and Kanzaki, S., Effects of rare-earth oxide and alumina additives on thermal conductivity of liquid-phase sintered silicon carbide. *J. Mater. Res.*, 2003, **18**, 1854–1862.
20. Le-Ngoc, L. and McCallion, H., A cellular finite element model for the cutting of softwood across the grain. *Int. J. Mech. Sci.*, 2000, **42**, 2283–2301.
21. Peters, C. C. and Cummin, J. D., Measuring wood surface smoothness: a review. *Forest. Prod. J.*, 1970, **20**(12), 40–43.
22. Heisel, U. and Tröger, J., Schnelle Beurteilung des Schneidkeilverleißes mittels Thermografie. *HOB - Die Holzbearbeitung*, 2002, **55**(1/2), 57–60.
23. Gogotsi, Y. G., Review—particulate silicon nitride-based composites. *J. Mater. Sci.*, 1994, **29**, 2541–2556.
24. Strakna, T. J., Jahanmir, S., Allor, R. L. and Kumar, K. V., Influence of grinding direction on fracture strength of silicon nitride. *J. Eng. Mater. Tech.*, 1996, **118**, 335–342.
25. Richter, K., Feist, W. C. and Knaebe, M. T., The effect of surface roughness on the performance of finishes. Part 1. Roughness characterization and stain performance. *Forest. Prod. J.*, 1995, **45**(7/8), 97.
26. Becher, P. F. and Ferber, M. K., Temperature-dependent viscosity of SiREAl-based glasses as a function of N:O and RE:Al ratios (RE = La, Gd, Y, and Lu). *J. Am. Ceram. Soc.*, 2004, **87**(7), 1274–1279.
27. Hampshire, S., Oxynitride glasses, their properties and crystallisation—a review. *J. Non-Cryst. Solids*, 2003, **316**, 64–73.
28. de Carvalho, M. C., da Silva, O. M. M., Strecker, K. and da Silva, C. R. M., The influence of nitrogen and argon atmospheres on the liquid phase sintering of silicon nitride. *Key Eng. Mat.*, 2001, **189–191**, 126–131.
29. Bodur, C. T., Szabó, D. V. and Kromp, K., Effects of heat treatment on the microstructure of yttria/alumina-doped hot-pressed silicon nitride ceramic. *J. Mater. Sci.*, 1993, **28**, 2089–2096.
30. Chollon, G., Vogt, U. and Berroth, K., Processing and characterization of an amorphous Si–N–(O) fibre. *J. Mater. Sci.*, 1998, **33**, 1529–1540.
31. Ziegler, A., McNaney, J. M., Hoffmann, M. J. and Ritchie, R. O., On the effect of local grainboundary chemistry on the macroscopic mechanical properties of a high-purity yttria–alumina containing silicon nitride ceramic: role of oxygen. *J. Am. Ceram. Soc.*, 2005, **88**(7), 1900–1908.